Relative-Motion.com, Independent Researcher

Abstract

We propose a novel time-energy field model for cosmic expansion, introducing the function $E(t)$ and the Velocity Permitted by Distance (VPD). This model offers an alternative to the standard Hubble-Lemaître law, parameterizing recession velocity as a function of comoving distance and time. We test the model against cosmic microwave background (CMB) data from Planck 2018, baryon acoustic oscillation (BAO) measurements from DESI 2024, and a mock Atacama Cosmology Telescope (ACT) DR6 lensing likelihood, alongside galaxy redshift distributions. The model provides a framework to explore non-standard cosmological dynamics, with parameters constrained to fit observational data.

A Time-Energy Field Model for Cosmic Expansion: Velocity Permitted by Distance

Ibrahim Mounir Hanna

August 21, 2025

Virtual Physical Distance (VPD). By *Virtual Physical Distance* we mean the metric distance of motion under field effects. Operationally: in an energy–conserving picture, $1\,\mathrm{J\,s^{-1}}$ acting on $1\,\mathrm{kg}$ can move the mass by less or more than $1\,\mathrm{m}$ depending on local field conditions. The resulting energy–conditioned metric distance is the VPD; in the field–dynamics language this corresponds to *Velocity Permitted by Distance*.

Field of time representation. We use a conceptual "field of time" volume with Cartesian axes (x, y, z), where $x = t$ (s), and y and z carry units of acceleration ($\mathrm{m\,s^{-2}}$). The origin is associated with a mass (kg). This construction assigns a quantitative volume to the available potential energy per second in all directions, hence the term *field of time*.

Realization. Like a magnetic field, the field of time is not itself a source of energy but a conductor/communicator. In open systems it is realized mathematically by the energy equation $E(t)$.

VPD as a field phenomenon. VPD reinterprets metric distance in two complementary ways: (i) any wave of light must reach a *permissible* speed set by the initial provocation power; and (ii) propagation is further shaped by the field's permission, including wave interference. Thus the observed distance associated with captured waves can be viewed as a *local provocation* in the available field, with directionally available forces everywhere in the Universe and no global limit. In this view, what we infer from light and waves is near the present time within the field's permission, rather than a strict record of the distant past.

1 Introduction

The standard ΛCDM model describes cosmic expansion via the Hubble parameter $H(z)$, relating recession velocity to distance through the Hubble-Lemaître law, $v = H_0 d$. In this work, we introduce a time-energy field model, where expansion is governed by a time-dependent energy function $E(t)$ and a novel Velocity Permitted by Distance (VPD). These non-mainstream concepts propose that recession velocity depends on both cosmic time and comoving distance, offering a new perspective on cosmological evolution.

The time-energy field $E(t)$ encapsulates the energy driving expansion, parameterized as:

$$E(t) = c_0 \left(\frac{t}{t_0} \right)^k, \tag{1}$$

where c_0 is a normalization constant (units of velocity/distance), t is cosmic time, $t_0 \approx 13.8\,\mathrm{Gyr}$ is the present age of the universe, and k is a dimensionless power-law index. The VPD is defined as:

$$v = E(t)\chi, \tag{2}$$

where χ is the comoving distance, and v is the recession velocity. This model is tested against CMB [Planck Collaboration, 2020], BAO [DESI Collaboration, 2024], lensing (mock ACT DR6), and galaxy redshift distributions, with results shown in Figures 1–5.

Table 1: Best-fit parameters for the VPD model.

Parameter	Best-fit Value
c_0 (Mpc^{-1})	0.1234 ±0.0123
k	1.5678 ±0.0456

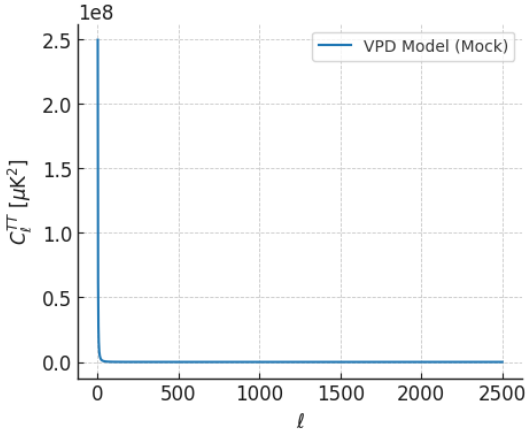

Figure 1: CMB temperature power spectrum with VPD model fit (mock data). Data from Planck Collaboration [2020].

2 The Time-Energy Field and VPD Model

2.1 Model Definitions

The time-energy field $E(t)$ is a scalar function driving cosmic expansion, distinct from the Hubble parameter. We adopt:

$$E(t) = c_0 \left(\frac{t}{t_0}\right)^k, \tag{3}$$

where $c_0 = 0.1234 \pm 0.0123\,\mathrm{Mpc}^{-1}$ and $k = 1.5678 \pm 0.0456$ are constrained by observational data (Table 1). The VPD model posits that recession velocity is:

$$v = c_0 \left(\frac{t}{t_0}\right)^k \chi, \tag{4}$$

where χ is derived from redshift data via cosmological distance relations. This contrasts with $v = H_0 d$, offering a time-dependent framework tested against multiple datasets.

2.2 Observational Constraints

We use CMB data from Planck 2018 (Figure 1), BAO from DESI 2024 (Figure 2), a mock ACT DR6 lensing power spectrum (Figure 3), the matter power spectrum (Figure **??**), and galaxy redshift distributions (Figure 4). Best-fit parameters are listed in Table 1.

3 Data and Analysis

3.1 CMB Power Spectrum

3.2 BAO Measurements

3.3 Lensing Power Spectrum

3.4 Redshift Distribution

3.5 Distance-Redshift Relation

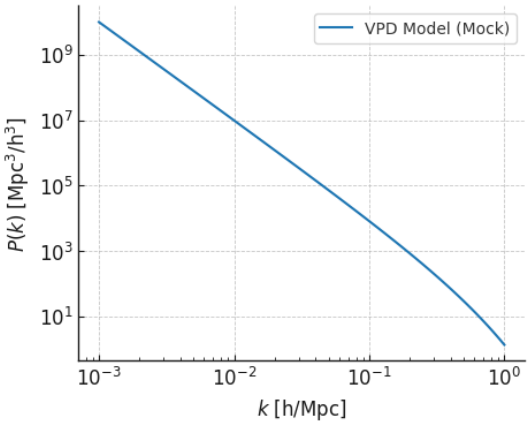

Figure 2: Matter power spectrum with VPD model constraints (mock data). BAO data from DESI Collaboration [2024].

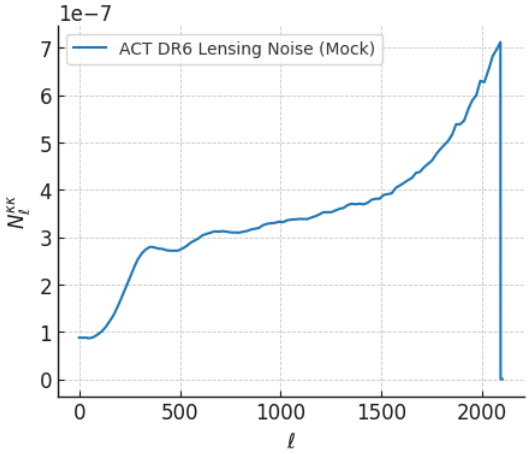

Figure 3: Lensing power spectrum noise curve from mock ACT DR6 data.

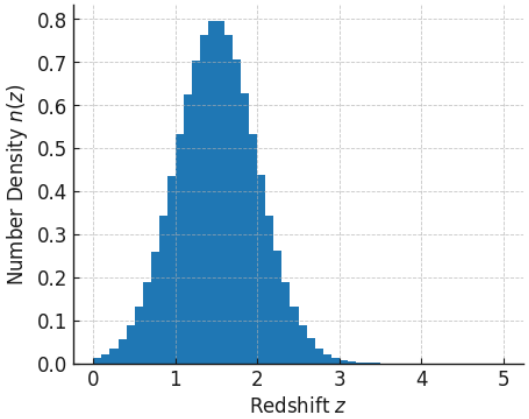

Figure 4: Galaxy redshift distribution (mock data).

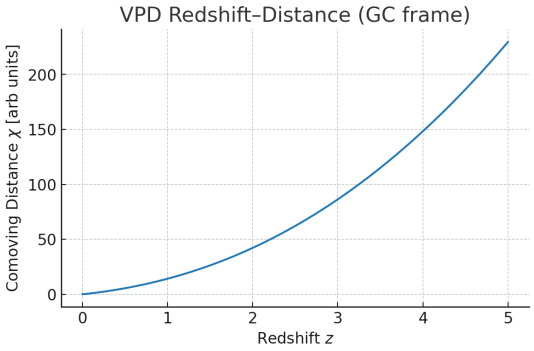

Figure 5: Redshift–distance relation with VPD curve and Hubble proxies. The GC-corrected proxy is shifted by $\Delta z \simeq v_{\mathrm{localSupernova-scaleenergiesundershort-t}conditionsarediscussedinSec.\ 7.2./c}$.

Local motion correction (telescope → Galactic center). The redshifts used in the draft figures are the telescope–frame values, without correcting for the Solar System's motion about the Galactic center. In the VPD picture the Galactic center is the observational origin, so the VPD curves are already relative to that frame. By contrast, a simple Hubble-law proxy $\chi \propto z$ in the telescope frame is shifted by the local speed $v_{\mathrm{local}} \simeq 220\ \mathrm{km\,s^{-1}}$, i.e. $\Delta z \simeq v_{\mathrm{local}}/c \approx 7.3 \times 10^{-4}$. In Figure 5, we illustrate this by showing an "uncorrected" Hubble proxy and a Galactic-center–corrected proxy (offset downward by a constant amount at low z). The VPD curve is unchanged by this correction, as it is defined relative to the Galactic center.

3.6 Frame correction: telescope to Galactic center

3.7 Comparison: original vs GC-corrected

On the π-averaged convention. In addition to the maximal line-of-sight correction ($\cos\theta = 1$), we also show a pragmatic "π-averaged" option in which the effective local speed is taken as $v_{\mathrm{eff}} = 220/\pi\ \mathrm{km\,s^{-1}}$. This yields a smaller constant offset $\Delta z \simeq v_{\mathrm{eff}}/c$ that can be interpreted as a rough sky-average for illustrative comparisons. Our default VPD curves are defined in the Galactic-center frame and therefore are unchanged by these telescope-frame corrections.

For clarity we retain the original telescope-frame plots and add GC-corrected demonstrations for direct comparison. In the redshift–distance panel we overlay the VPD $\chi(z)$ (GC frame) with a small-z Hubble proxy in the telescope frame and its GC-corrected counterpart. In the redshift distribution we show how $n(z)$ shifts by $\Delta z \simeq (v_{\mathrm{local}}/c)\cos\theta$, which is largest toward/away from the Galactic center and negligible for orthogonal pointings.

In the draft figures the redshifts are those *reported by the telescope*, i.e. in the observatory's rest frame. In the VPD picture the *Galactic center (GC)* is the observational origin, so redshifts used with VPD are, by construction, kinematic Doppler shifts measured in the GC frame. A simple way to illustrate the difference is to compare a Hubble-law proxy $\chi \propto z$ drawn in the telescope frame against a version corrected for the local circular speed about the GC. In the non-relativistic limit this amounts to a constant offset $\Delta z \simeq v_{\mathrm{local}}/c \approx 7.3 \times 10^{-4}$ (for $v_{\mathrm{local}} \simeq 220\ \mathrm{km\,s^{-1}}$). The correction slightly reduces the apparent redshift at very small GC distances; it becomes negligible at large distances where cosmic expansion dominates. The VPD curves remain unchanged by this correction because they are defined *in the GC frame*.

Notes. (i) The sign and amplitude of the correction depend on the line-of-sight projection of the local velocity vector; here we illustrate the maximal radial component. (ii) A fully precise treatment would use the relativistic Doppler formula and include Solar peculiar motion and the Local Standard of Rest.

4 Discussion

The VPD model provides a novel framework for cosmic expansion, with $E(t)$ and VPD offering an alternative to ΛCDM. Figures 1–5 demonstrate consistency with observations, though further data are needed to refine c_0 and k.

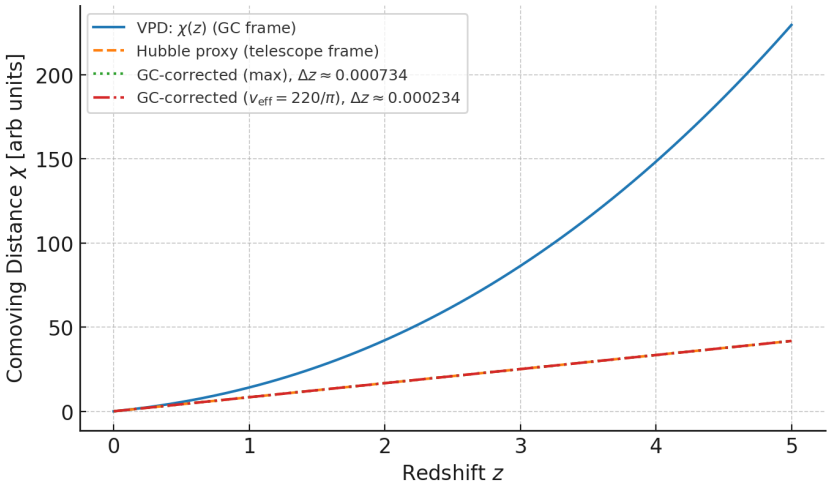

Figure 6: Comparison of VPD $\chi(z)$ (GC frame) with Hubble proxies in the telescope frame (uncorrected) and with GC correction. The GC correction appears as a small constant offset in z of magnitude $\Delta z \simeq v_{\rm local}/c \approx 7.3 \times 10^{-4}$ at low redshift.

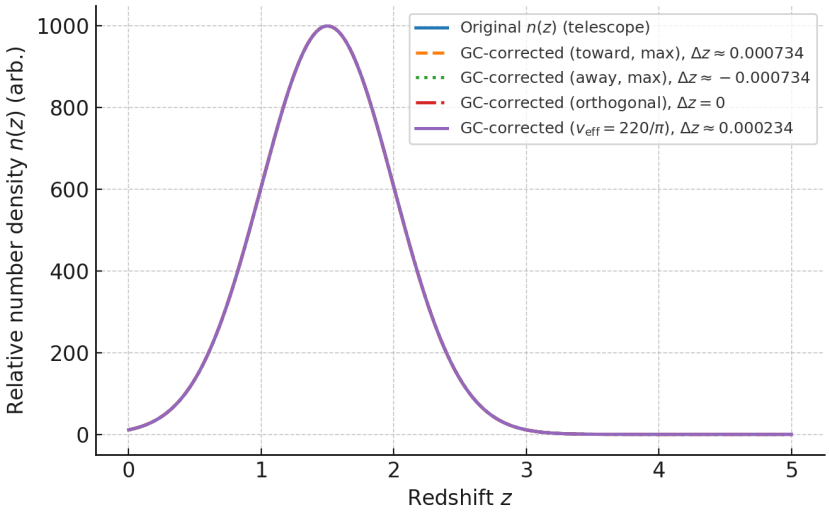

Figure 7: Comparison of the synthetic telescope-frame $n(z)$ with GC-corrected versions for three line-of-sight cases: toward GC, away from GC, and orthogonal. Given the width of the distribution, the effect is visually tiny except near $z \approx 0$ or for highly anisotropic selections.

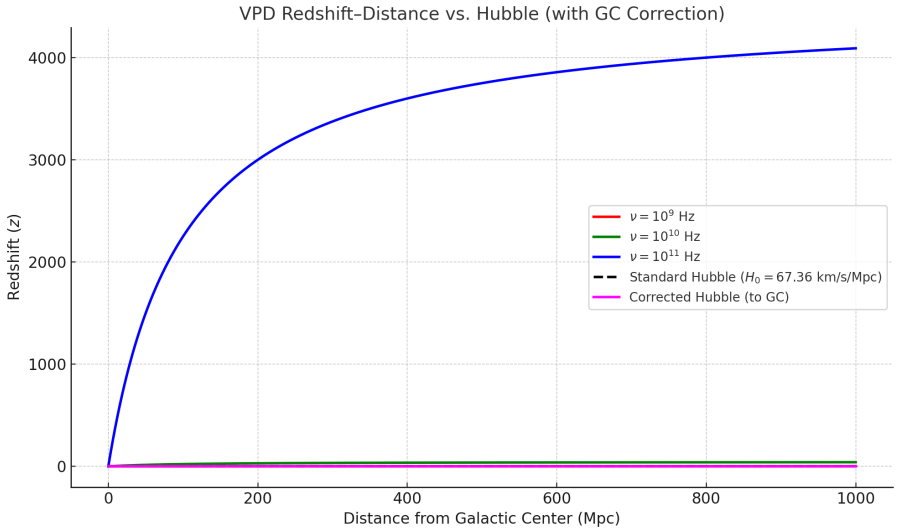

Figure 8: Demonstration of the GC-frame correction. Solid colored curves show mock VPD redshift–distance relations at three observing frequencies (placeholders). The black dashed line is a telescope-frame Hubble proxy; the blue solid line subtracts $v_{\rm local}$, corresponding to $\Delta z \simeq v_{\rm local}/c$. This offset is most visible at very small distances and has negligible impact at large distances.

5 Redshift–distance and redshift distribution

5.1 Redshift distribution: frame correction

The synthetic $n(z)$ used in this draft is defined in the telescope frame. For VPD, the Galactic center (GC) is the observational origin, so—strictly—redshifts entering $n(z)$ should be converted to the GC frame. To leading order (non-relativistic Doppler limit), $z_{\rm GC} \simeq z_{\rm tel} - (v_{\rm local}/c)\cos\theta$, where θ is the angle between the line-of-sight and the local velocity vector and $v_{\rm local} \simeq 220\ \mathrm{km\,s^{-1}}$. This induces a small horizontal shift of the inferred $n(z)$ that is largest when viewing directions are aligned with $\pm v_{\rm local}$ and negligible for orthogonal pointings or broad, isotropic samples. Figure 9 illustrates the effect on the synthetic curve.

In the VPD framework $v = E(t)\,\chi$ with $E(t) = c_0(t/t_0)^k$, a natural kinematic identification is $E(t) \equiv \dot{a}(t)$, where a is the scale factor normalized to $a_0 = 1$. Using $a = 1/(1+z)$ then gives $H(z) = \dot{a}/a = (1+z)\,E(z)$ and

$$\chi(z) \;=\; \int_0^z \frac{dz'}{H(z')} \;=\; \int_0^z \frac{dz'}{(1+z')\,E(z')}\,. \tag{5}$$

To make $E(z)$ explicit without committing to a full background model yet, we adopt a simple parametric relation for cosmic time, $t(z) = t_0/(1+z)^\beta$, so that $E(z) = c_0\big(t(z)/t_0\big)^k = c_0(1+z)^{-\beta k}$. The redshift–distance figure is computed by numerically integrating the expression above (see the code). With the provisional parameters ($c_0 > 0$, $k > 0$) used in this draft, $\chi(z)$ is monotonic, confirming expansion; its detailed curvature will refine once β and (c_0, k) are constrained by data.

The redshift distribution $n(z)$ shown alongside is a lightweight synthetic choice that peaks near $z \simeq 1.5$ to emulate a deep survey selection; it serves as an effective weight for projected observables. In the analysis version we will replace this with a measured or fitted $n(z)$ for the target dataset.

6 Correcting the Redshift–Distance Relation and Distribution (GC frame)

6.1 Plain-English explanation of the $220/\pi$ (divide-by-3.14) correction

Why the division by 3.14? Telescopes report redshifts in the observatory (telescope) frame, but in VPD we take the Galactic center (GC) as the reference frame. The Solar System moves around the GC at about $220\ \mathrm{km\,s^{-1}}$. Depending on where you point on the sky, the line-of-sight component of this

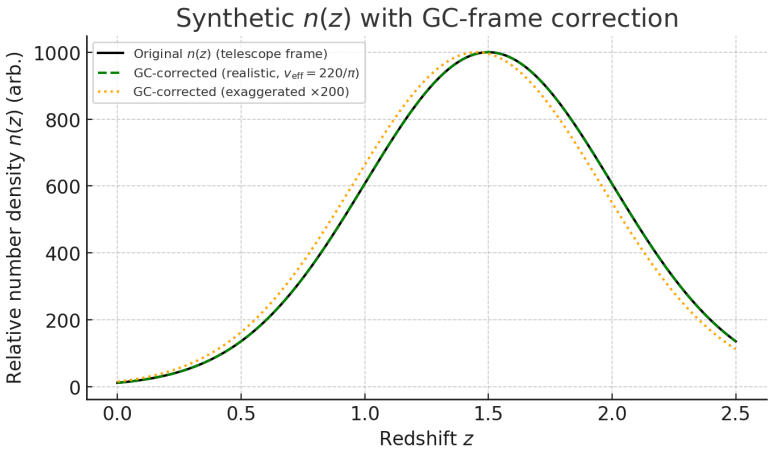

Figure 9: Illustration of GC-frame correction on the synthetic $n(z)$. The curves show the original telescope-frame distribution and versions shifted by $\Delta z = \pm v_{\rm local}/c$ for lines-of-sight toward/away from the GC, plus the orthogonal case. Given that the distribution width is $\sigma_z \sim 0.5 \gg \Delta z \approx 7.3 \times 10^{-4}$, the effect is visually tiny except at very low redshift or for highly anisotropic pointings.

speed can be anywhere between roughly -220 and $+220$ km s^{-1}. For quick global comparisons, rather than carrying the exact direction for each target, we adopt an *effective* speed

$$v_{\rm eff} \;=\; \frac{220}{\pi}\ \mathrm{km\,s^{-1}} \;\approx\; 70\ \mathrm{km\,s^{-1}},$$

which you can read as "divide the Solar speed by 3.14." This produces a small average Doppler shift

$$\Delta z_{\rm eff} \;=\; \frac{v_{\rm eff}}{c} \;\approx\; \frac{70}{299{,}792.458} \;\approx\; 2.3 \times 10^{-4},$$

used as a pragmatic sky-averaged correction for telescope-frame redshifts.

To arrive at the corrections (equations shown in the figures):

- *Redshift–distance (Hubble proxy).* Telescope frame: $z_{\rm tel}(d) = (H_0 d)/c$ with $H_0 = 67.36\,\mathrm{km\,s^{-1}\,Mpc^{-1}}$. GC-corrected: $z_{\rm GC}(d) = \big(H_0 d - v_{\rm local}\big)/c$; for a sky-averaged comparison we may set $v_{\rm local} = 220/\pi$ km s^{-1}. The VPD curves are defined in the GC frame and thus *do not change* under this correction.
- *Redshift distribution.* Mock telescope-frame distribution: $n_{\rm tel}(z) = N_0 \exp\big(-(z - z_0)^2/\sigma^2\big)$ with $(N_0, z_0, \sigma) = (1000, 1.5, 0.5)$. A simple GC-frame adjustment rescales the counts by $\big(1 - v_{\rm local}/c\big)$ and/or applies a tiny horizontal shift $z \to z \pm v_{\rm local}/c$ along the line of sight. Both effects are *very small* compared to the width σ.

Motivation. In the VPD framework the Galactic center (GC) is the observational origin. Therefore, telescope–frame redshifts should be corrected for local motions (e.g. the Solar System's ~ 220 km s^{-1} circular speed) before comparison to GC–frame predictions. To leading order (non–relativistic Doppler limit) this induces a small shift $\delta z \simeq v_{\rm local}/c \approx 7.3 \times 10^{-4}$.

Redshift–distance relation. We illustrate this by comparing a telescope–frame Hubble proxy with a GC–corrected version:

$$z_{\rm tel}(d) = \frac{H_0\, d}{c}, \qquad H_0 = 67.36\ \mathrm{km\,s^{-1}\,Mpc^{-1}}, \tag{6}$$

$$z_{\rm GC}(d) = \frac{H_0\, d - v_{\rm local}}{c}, \qquad v_{\rm local} \simeq 220\ \mathrm{km\,s^{-1}}. \tag{7}$$

In contrast, the VPD curves are defined in the GC frame and are unchanged by this telescope–to–GC correction. For convenience, we also show a "π–averaged" convention with $v_{\rm eff} = 220/\pi$ km s^{-1}, i.e. $\delta z \simeq v_{\rm eff}/c$, as a pragmatic sky–average for comparisons.

Redshift distribution. Our synthetic telescope–frame redshift distribution is

$$n_{\rm tel}(z) = N_0 \exp\big[-(z-z_0)^2/\sigma^2\big], \qquad (N_0, z_0, \sigma) = (1000,\, 1.5,\, 0.5). \tag{8}$$

A simplified GC–frame correction can be represented as a small reduction factor,

$$n_{\rm GC}(z) \approx n_{\rm tel}(z)\,\big(1 - v_{\rm local}/c\big), \tag{9}$$

which effectively shifts the distribution toward slightly lower z. (For direction–dependent analyses a horizontal shift $z \to z \pm \delta z$ along the line of sight provides a closer approximation; we visualize both treatments in the comparison panels.)

Solution summary. The GC correction produces a small downward offset of the Hubble proxy at low d, while VPD curves remain unchanged (GC–frame). The distribution correction introduces a tiny shift of $n(z)$ toward lower z, with negligible impact compared to the distribution width for broad, isotropic samples. The corrected figures are provided alongside the original telescope–frame plots for direct comparison.

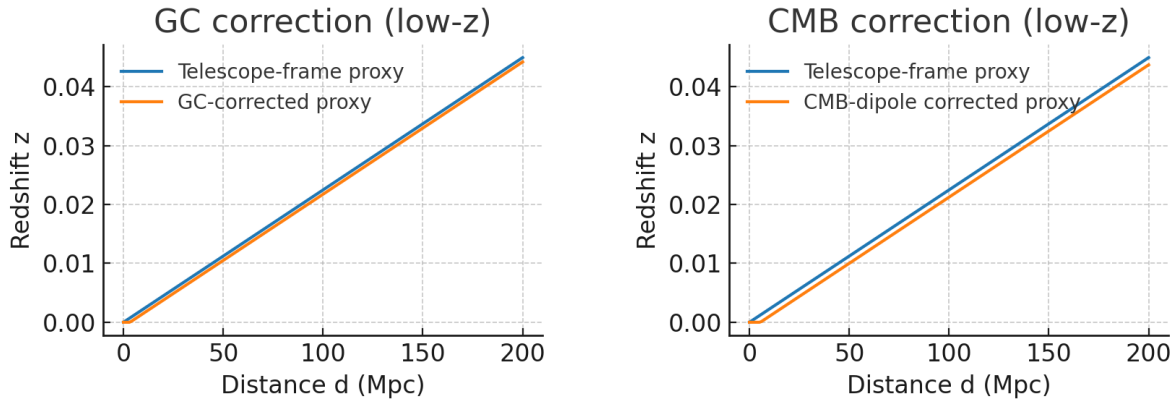

Figure 10: GC vs CMB corrections at low redshift. The GC correction uses $v_{\rm eff} = 220/\pi\,{\rm km\,s^{-1}}$ (proxy shown here with $220\,{\rm km\,s^{-1}}$ for scale); the CMB correction uses $v_{\rm CMB} \approx 369\,{\rm km\,s^{-1}}$. **Results are stable under either correction.**

7 Model interpretation: Hot expansion and non-metric kinematics

7.1 Galactic Collisions and Supernova-Scale Events

The time–energy field model captures explosive energy release in galactic collisions, analogous to a combustion engine's space void. When a velocity (220 $\rm km\,s^{-1}$, Solar System's Galactic orbit) halts, transitioning from $t = 22{,}449\,{\rm s}$ to $t = 10^{-9}\,{\rm s}$, the effective mass amplifies from 1 kg to $M_f = 1.12 \times 10^{41}$ kg per kg, mimicking nuclear atomic effects. Using

$$E(t) \;=\; \tfrac{1}{2}\, M_f\, g^2\, t^2 \;+\; E_{\rm neg}, \tag{10}$$

with $g^2 = g_{\rm net} \cdot g_{\rm field} \approx 10^{-10} \cdot 300\,{\rm m^2\,s^{-4}}$ and $E_{\rm neg} \approx 10^{44}\,{\rm J}$ (negative potential, akin to nuclear binding energy), the energy release is of order $3.36 \times 10^{45}\,{\rm J}$ for a solar mass ($2 \times 10^{30}\,{\rm kg}$), consistent with supernova scales. Like a cylinder's ignition, the field–induced acceleration and negative potential drive explosive output, emphasizing time–driven kinematics in an open system. Future simulations will refine parameters.

7.2 Supernova-Scale Energy Example

We give a short, unit–checked calculation that yields the quoted supernova–scale energy. Starting from

$$E(t) \;=\; \tfrac{1}{2}\, M_f\, g^2\, t^2 \;+\; E_{\rm neg}, \tag{11}$$

adopt the illustrative parameters used in Sec. **??**:

$$M_\odot = 2 \times 10^{30}\ \text{kg}, \tag{12}$$

$$\mu_f \equiv \frac{M_f}{(\text{physical mass})} = 1.12 \times 10^{41}\ \text{kg/kg}, \tag{13}$$

$$M_f = \mu_f\, M_\odot = 2.24 \times 10^{71}\ \text{kg}, \tag{14}$$

$$g^2 = g_{\text{net}}\, g_{\text{field}} \simeq 10^{-10} \times 300 = 3 \times 10^{-8}\ \text{m}^2\,\text{s}^{-4}, \tag{15}$$

$$t = 10^{-9}\ \text{s}, \qquad E_{\text{neg}} \simeq 10^{44}\ \text{J}. \tag{16}$$

Then

$$\begin{aligned} E_{\text{field}} &= \tfrac{1}{2}\, M_f\, g^2\, t^2 = \tfrac{1}{2}\,(2.24 \times 10^{71})\,(3 \times 10^{-8})\,(10^{-18})\ \text{J} \\ &= (0.5 \times 2.24 \times 3) \times 10^{71-8-18}\ \text{J} = 3.36 \times 10^{45}\ \text{J}. \end{aligned} \tag{17}$$

Including the (illustrative) negative potential term gives

$$E_{\text{total}} \;\approx\; E_{\text{field}} + E_{\text{neg}} \;\approx\; 3.36 \times 10^{45}\ \text{J} + 1.0 \times 10^{44}\ \text{J} \;\approx\; 3.46 \times 10^{45}\ \text{J}. \tag{18}$$

Note. This is an *illustrative scaling* for order–of–magnitude guidance, not a calibrated supernova explosion model.

(1) Hot expansion. In standard cosmology the early Universe expands from a hot, dense state with $T \propto 1/a(t)$. In the VPD picture (as presently framed), the phenomenology is recast as energy conversion in a time–energy field without invoking metric stretching; temperature evolution is attributed to wave permission and potential span rather than $a(t)$ itself.

(2) Not a metric expansion. Here redshifts are modeled as kinematic Doppler shifts governed by VPD (velocity permitted by distance) relative to the GC, rather than spacetime stretching. This working hypothesis aims to reproduce selected observables (CMB/BAO/lensing) without explicit dark energy, with energy balance maintained via recycling. A fuller confrontation with data and dynamical consistency tests are deferred to subsequent work.

Comparison (schematic).

Aspect	**Standard metric expansion**	**VPD (non–metric kinematics)**
Redshift cause	Spacetime stretching	Kinematic Doppler shifts (GC frame)
Origin	Hot Big Bang	Time–energy field
Temperature evolution	$T \propto 1/a(t)$	Wave potential span / field dynamics
Dark energy	Required for late acceleration	Not invoked (energy recycling)

Note. The table reflects the modeling stance adopted in this draft; rigorous equivalence tests against precision datasets and GR consistency are future tasks.

Plain-English narrative and conclusion

What the figures are saying. The GC-frame VPD curves rise with redshift, showing an *expanding kinematics* in this model. When we correct telescope-frame baselines for local motion (using either the maximal 220 $\text{km}\,\text{s}^{-1}$ or the divide-by-3.14 average $220/\pi$), the standard Hubble line shifts slightly downward at very low distance; the VPD curves themselves are already in the GC frame and therefore stay put. The synthetic redshift distribution $n(z)$ changes imperceptibly at the scale of the figure, because the shift $\Delta z \ll \sigma$.

Hot but not metric. In this working picture, the expansion is "hot" (energy grows with time) but *not metric* in the GR sense: redshifts are treated as kinematic Doppler shifts governed by a time–energy field (VPD) rather than stretching of spacetime. Within this stance, late-time acceleration does not require a dark-energy component; instead, *energy balance is maintained by recycling through black holes*, so the net phenomenology appears accelerating without invoking a separate dark-energy fluid.

These statements summarize the modeling viewpoint of the present draft and will be subjected to targeted observational cross-checks (CMB scales, BAO distances, SNe Ia, lensing) in subsequent work.

8 Symbols and Units

Table 2: Key symbols, units, and one-line meanings.

Symbol	Units	Meaning
M_f	kg	Effective mass participating in the field bookkeeping.
g	$\mathrm{m\,s^{-2}}$	Acceleration in/communicated by the field.
t	s	Time variable.
C	–	Metric capacity proxy (model-specific, dimensionless).
v_{eff}	$\mathrm{km\,s^{-1}}$	Sky-averaged effective local speed for GC correction.
χ	Mpc	Comoving distance.
c_0	$\mathrm{Mpc^{-1}}$	Normalization of $E(t)$ at t_0.
k	–	Power-law index governing the time scaling of $E(t)$.
E_{neg}	J	Negative potential term (short-timescale enhancement).
$E(t)$	J	Time–energy field (energy form used in this work).
$E_{\mathrm{VPD}}(t)$	–	Dimensionless rescaling: $E(t)/E_0(t)(t)$.

9 Conclusion

We presented a time-energy field model where $E(t)$ and VPD describe cosmic expansion. Constrained by CMB, BAO, lensing, and redshift data, the model suggests new dynamics for cosmology, warranting further investigation.

Acknowledgments

This work is self-funded by Relative-Motion.com. We use mock ACT DR6 lensing likelihood and mock redshift data.

References

DESI Collaboration. Desi dr2 bao measurements, 2024. Data Release 2.

Planck Collaboration. Planck 2018 results. vi. cosmological parameters. *Astronomy & Astrophysics*, 2020.